WCAP 10976
Revision 2

TECHNICAL BASES FOR ELIMINATING LARGE PRIMARY LOOP PIPE RUPTURE AS THE STRUCTURAL DESIGN BASIS FOR INDIAN POINT UNIT 2
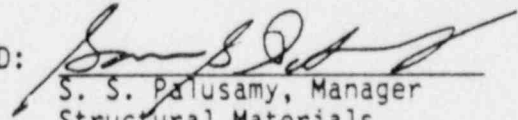
Original: November, 1985
Revision 1:   March, 1986
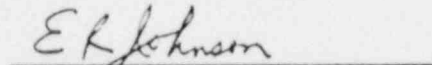Revision 2:   December, 1986

B. A. Bishop   F. J. Witt
S. A. Swamy   S. R. Nelson
Y. S. Lee   H. F. Clark, Jr.
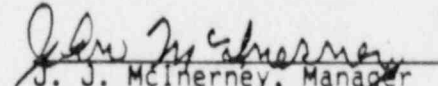
VERIFIED: J. C. Schmertz

APPROVED: _____
S. S. Palusamy, Manager
Structural Materials
Engineering

APPROVED: _E. R. Johnson_____
E. R. Johnson, Manager
Structural and Seismic
Development

APPROVED: _____
J. J. McInerney, Manager
Mechanical Equipment and
Systems Licensing

WESTINGHOUSE ELECTRIC CORPORATION
Nuclear Energy Systems
P. O. Box 2728
Pittsburgh, Pennsylvania 15230-2728

FOREWORD

This document contains Westinghouse Electric Corporation proprietary information and data which has been identified by brackets. Coding associated with the brackets sets forth the basis on which the information is considered proprietary. These codes are listed with their meanings in WCAP-7211.

The proprietary information and data contained in this report were obtained at considerable Westinghouse expense and its release could seriously affect our competitive position. This information is to be withheld from public disclosure in accordance with the Rules of Practice 10 CFR 2.790 and the information presented herein be safeguarded in accordance with 10 CFR 2.903. Withholding of this information does not adversely affect the public interest.

This information has been provided for your internal use only and should not be released to persons or organizations outside the Directorate of Regulation and the ACRS without the express written approval of Westinghouse Electric Corporation. Should it become necessary to release this information to such persons as part of the review procedure, please contact Westinghouse Electric Corporation, which will make the necessary arrangements required to protect the Corporation's proprietary interests.

The proprietary information is deleted in the unclassified version of this report (WCAP-10976, Revision 2).

Revision 1 of this report was dated March 1986. Since that time significant revisions were made to the prime reference document WCAP-10931 (now WCAP-10931, Revision 1 and Reference 21 of this document) wherefrom revised end-of-service life toughness criteria were established. These new criteria required that additional analyses be performed and evaluations made, hence prompting the revision of this report. The revisions are identified by vertical lines in the margin.

TABLE OF CONTENTS

LIST OF TABLES

LIST OF FIGURES

LIST OF FIGURES (Cont'd.)

1.0 SUMMARY AND INTRODUCTION

1.1 Summary

The structural design basis for the reactor coolant system primary loop requires that pipe breaks be postulated. However such breaks have been shown to be highly unlikely on a generic basis and the Nuclear Regulatory Commission is receptive to exemption requests for considering breaks on a plant specific basis. In this report the applicability of the generic evaluations to the Indian Point Unit 2 piping system is demonstrated by presenting a fracture mechanics evaluation, a determination of leak rates from a through-wall crack, a fatigue crack growth evaluation and an assessment of margins.

Major emphasis is on the cast fittings which are limiting. Geometries, loadings and heat chemistries are summarized. Fracture toughness values are established for each fitting using the alternate toughness criteria approach. Fracture mechanics and leak rate calculations showed that acceptable margins exist between cracks which are stable and those for which detectable leak rates are demonstrated.

The major conclusions is that reactor coolant system primary loop pipe breaks need not be considered in the structural design basis of the Indian Point Unit 2 plant.

1.2 Introduction

1.2.1 Purpose

This report applies to the Indian Point Unit 2 Reactor Coolant System (RCS) primary loop piping. It is intended to demonstrate that for the specific parameters of the Indian Point plant, RCS primary loop pipe breaks need not be considered in the structural design basis. The approach taken has been accepted by the Nuclear Regulatory Commission (NRC) (Reference 1).

1.2.2 Scope

The structural design basis for the RCS primary loop requires that pipe breaks be postulated. In addition, protective measures for the dynamic effects associated with RCS primary loop pipe breaks have been incorporated in the Indian Point Unit 2 plant design. However, Westinghouse has demonstrated on a generic basis that RCS primary loop pipe breaks are highly unlikely and should not be included in the structural design basis of Westinghouse plants (see Reference 2). In order to demonstrate this applicability of the generic evaluations to the Indian Point plant, Westinghouse has performed a fracture mechanics evaluation, a determination of leak rates from a through-wall crack, a fatigue crack growth evaluation, and an assessment of margins.

1.2.3 Objectives

In order to validate the elimination of RCS primary loop pipe breaks for the Indian Point Unit 2 plant, the following objectives must be achieved:

a. Demonstrate that margin exists between the "critical" crack size and a postulated crack which yields a detectable leak rate.

b. Demonstrate that there is sufficient margin between the leakage through a postulated crack and the leak detection capability of the Indian Point plant.

c. Demonstrate that fatigue crack growth is negligible.

1.2.4 Background Information

Westinghouse has performed considerable testing and analysis to demonstrate that RCS primary loop pipe breaks can be eliminated from the structural design basis of all Westinghouse plants. The concept of eliminating pipe breaks in the RCS primary loop was first presented to the NRC in 1978 in WCAP-9283 (Reference 3). That Topical Report employed a deterministic fracture mechanics evaluation and a probabilistic analysis to support the elimination

of RCS primary loop pipe breaks. That approach was then used as a means of addressing Generic Issue A-2 and Asymmetric LOCA Loads.

Westinghouse performed additional testing and analysis to justify the elimination of RCS primary loop pipe breaks. This material was provided to the NRC along with Letter Report NS-EPR-2519 (Reference 4).

The NRC funded research through Lawrence Livermore National Laboratory (LLNL) to address this same issue using a probabilistic approach. As part of the LLNL research effort, Westinghouse performed extensive evaluations of specific plant loads, material properties, transients, and system geometries to demonstrate that the analysis and testing previously performed by Westinghouse and the research performed by LLNL applied to all Westinghouse plants including Indian Point (References 5 and 6). The results from the LLNL study were released at a March 28, 1983 ACRS Subcommittee meeting. These studies which are applicable to all Westinghouse plants east of the Rocky Mountains determined the mean probability of a direct LOCA (RCS primary loop pipe break) to be 10^{-10} per reactor year and the mean probability of an indirect LOCA to be 10^{-7} per reactor year. Thus, the results previously obtained by Westinghouse (Reference 3) were confirmed by an independent NRC research study.

Based on the studies by Westinghouse, LLNL, the ACRS, and the AIF, the NRC completed a safety review of the Westinghouse reports submitted to address asymmetric blowdown loads that result from a number of discrete break locations on the PWR primary systems. The RC Staff evaluation (Reference 1) concludes that an acceptable technical basis has been provided so that asymmetric blowdown loads need not be considered for those plants that can demonstrate the applicability of the modeling and conclusions contained in the Westinghouse response or can provide an equivalent fracture mechanics demonstration of the primary coolant loop integrity.

This report provides a fracture mechanics demonstration of primary loop integrity for the Indian Point Unit 2 plant consistent with the NRC position for not considering asymmetric blowdown.

2.0 OPERATION AND STABILITY OF THE REACTOR COOLANT SYSTEM

The Westinghouse reactor coolant system primary loop has an operating history which demonstrates the inherent stability characteristics of the design. This includes a low susceptibility to cracking failure from the effects of corrosion (e.g., intergranular stress corrosion cracking), water hammer, or fatigue (low and high cycle). This operating history totals over 450 reactor-years, including five plants each having 16 years of operation and 15 other plants each with over 11 years of operation.

2.1 Stress Corrosion Cracking

For the Westinghouse plants, there is no history of cracking failure in the reactor coolant system loop piping. For stress corrosion cracking (SCC) to occur in piping, the following three conditions must exist simultaneously: high tensile stresses, a susceptible material, and a corrosive environment (Reference 7). Since some residual stresses and some degree of material susceptibility exist in any stainless steel piping, the potential for stress corrosion is minimized by proper material selection immune to SCC as well as preventing the occurrence of a corrosive environment. The material specifications consider compatibility with the system's operating environment (both internal and external) as well as other materials in the system, applicable ASME Code rules, fracture toughness, welding, fabrication, and processing.

The environments known to increase the susceptibility of austenitic stainless steel to stress corrosion are (Reference 7): oxygen, fluorides, chlorides, hydroxides, hydrogen peroxide, and reduced forms of sulfur (e.g., sulfides, sulfites, and thionates). Strict pipe cleaning standards prior to operation and careful control of water chemistry during plant operation are used to prevent the occurrence of a corrosive environment. Prior to being put into service, the piping is cleaned internally and externally. During flushes and preoperational testing, water chemistry is controlled in accordance with written specifications. External cleaning for Class 1 stainless steel piping includes patch tests to monitor and control chloride and fluoride levels. For

preoperational flushes, influent water chemistry is controlled. Requirements on chlorides, fluorides, conductivity, and pH are included in the acceptance criteria for the piping.

During plant operation, the reactor coolant water chemistry is monitored and maintained within very specific limits. Contaminant concentrations are kept below the thresholds known to be conducive to stress corrosion cracking with the major water chemistry control standards being included in the plant operating procedures as a condition for plant operation. For example, during normal power operation, oxygen concentration in the RCS is expected to be less than 0.005 ppm by controlling charging flow chemistry and maintaining hydrogen in the reactor coolant at specified concentrations. Halogen concentrations are also stringently controlled by maintaining concentrations of chlorides and fluorides within the specified limits. This is assured by controlling charging flow chemistry and specifying proper wetted surface materials.

2.2 Water Hammer

Overall, there is a low potential for water hammer in the RCS since it is designed and operated to preclude the voiding condition in normally filled lines. The reactor coolant system, including piping and primary components, is designed for normal, upset, emergency, and faulted condition transients. The design requirements are conservative relative to both the number of transients and their severity. Relief valve actuation and the associated hydraulic transients following valve opening are considered in the system design. Other valve and pump actuations are relatively slow transients with no significant effect on the system dynamic loads. To ensure dynamic system stability, reactor coolant parameters are stringently controlled. Temperature during normal operation is maintained within a narrow range by control rod position; pressure is controlled by pressurizer heaters and pressurizer spray also within a narrow range for steady-state conditions. The flow characteristics of the system remain constant during a fuel cycle because the only governing parameters, namely system resistance and the reactor coolant pump characteristics, are controlled in the design process. Additionally, Westinghouse has instrumented typical reactor coolant systems to verify the

flow and vibration characteristics of the system. Preoperational testing and operating experience have verified the Westinghouse approach. The operating transients of the RCS primary piping are such that no significant water hammer can occur.

2.3 Low Cycle and High Cycle Fatigue

Low cycle fatigue considerations are accounted for in the design of the piping system through the fatigue usage factor evaluation to show compliance with the rules of Section III of the ASME Code. A further evaluation of the low cycle fatigue loadings was carried out as part of this study in the form of a fatigue crack growth analysis, as discussed in Section 6.

High cycle fatigue loads in the system would result primarily from pump vibrations. These are minimized by restrictions placed on shaft vibrations during hot functional testing and operation. During operation, an alarm signals the exceedance of the vibration limits. Field measurements have been made on a number of plants during hot functional testing, including plants similar to Indian Point Unit 2. Stresses in the elbow below the reactor coolant pump have been found to be very small, between 2 and 3 ksi at the highest. These stresses are well below the fatigue endurance limit for the material and would also result in an applied stress intensity factor below the threshold for fatigue crack growth.

3.0 PIPE GEOMETRY AND LOADING

The general analytical approach is discussed first. A segment of the primary
coolant hot leg pipe shown below to be limiting in terms of stresses is
sketched in Figure 3-1. This segment is postulated to contain a
circumferential through-wall flaw. The inside diameter and wall thickness of
the pipe are 29.2 and 2.69 inches, respectively. The pipe is subjected to a
normal operating pressure of 2235 psi. Figure 3-2 identifies the loop weld
locations. The material properties and the loads at these locations resulting
from deadweight, thermal expansion, and Safe Shutdown Earthquake are indicated
in Table 3-1. As seen from this table, the junction of the hot leg and the
reactor vessel outlet nozzle is the worst location for crack stability
analysis based on the highest stress due to combined pressure, dead weight,
thermal expansion, and SSE (Safe Shutdown Earthquake) loadings. At this
location, the axial load (F_x) and the bending moment (M_b) are 1768 kips
(including axial force due to pressure) and 38,913 in-kips, respectively. This
location will be referred to as the load critical location. However, as seen
later, significant degradation of end-of-service life fracture toughnesses due
to thermal aging occurs in several pipe fittings. The highest stressed weld
location for which a pipe fitting suffers such degradation will be referred to
as a toughness critical location. The associated heat of material will be
called the toughness critical material. As seen in Table 3-1, the toughness
critical locations are 3, 4, 9, and 12 (see Figure 3-2).

The loads of Table 3-1 are calculated as follows: The axial force F and
transverse bending moments, M_y and M_z, are chosen for each static load
(pressure, deadweight, and thermal) based on elastic-static analyses for each
of these load cases. These pipe load components are combined algebraically to
define the equivalent pipe static loads F_s, M_{ys}, and M_{zs}. Based on
elastic SSE response spectra analyses, amplified pipe seismic loads, F_d,
M_{yd}, M_{zd}, are obtained. The maximum pipe loads are obtained by combining
the static and dynamic load components as follows:

$$F_x = |F_s| + |F_d|$$

$$M_b = \sqrt{M_y^2 + M_z^2}$$

where:

$$M_y = |M_{ys}| + |M_{yd}|$$

$$M_z = |M_{zs}| + |M_{zd}|$$

The normal operating loads (i.e., algebraic sum of pressure, deadweight, and 100 percent power thermal expansion loading) at the locations identified in Figure 3-2 are given in Table 3-2. The loads were determined as described above.

The calculated and allowable stresses for ASME III NB-3600 equation 9 (faulted i.e., pressure, deadweight, and SSE) and equation 12 (normal operating thermal stress) at load critical location 1 are as follows:

Equation Number	Calculated Stress (ksi)	Allowable Stress (ksi)	Ratio of Calculated/ Allowable
9F	12.3	50.1	0.25
12	15.8	50.1	0.32

At the other locations, the calculated stresses and ratios are even less.

TABLE 3-1

INDIAN POINT UNIT 2 PRIMARY LOOP DATA INCLUDING FAULTED LOADING CONDITIONS

Weld Locations	Inside Radius (in)	Wall Thickness (in)	Yield Stress σ_y (ksi)	Ultimate Stress σ_u (ksi)	Flow Stress $[\quad]^{a,c,e}$ (ksi)	Faulted Loads[a] Axial Load (Kips) F_x	Bending Moment (in-Kips) M_b	Direct Stress (ksi) $\sigma_a = \frac{F_x}{A} + \frac{M_b}{Z}$
1[b]	14.6	2.69	18.7	71.8	45.2	1768	38913	26.0
2	14.6	2.69	18.7	67.0	42.8	1767	14511	13.8
3[c]	15.6	2.88	18.7	67.0	42.8	1724	23661	15.3
4[c]	15.6	2.88	19.4	67.0	43.2	1715	24896	15.8
5	15.6	2.88	19.4	67.0	43.2	1591	10725	9.6
6	15.6	2.88	19.4	67.0	43.2	1589	6844	8.0
7	15.6	2.88	19.4	67.0	43.2	1841	12131	1'.0
8	15.6	2.88	19.4	67.0	43.2	1836	17292	13 1
9[c]	15.6	2.88	19.4	67.0	43.2	1940	29460	18 4
10	13.85	2.55	19.4	71.8	45.6	1690	16381	16.6
11	13.85	2.55	19.4	67.0	43.2	1693	8883	12.2
12[c]	13.85	2.55	19.4	67.0	43.2	1664	9627	12.5

---

[a]Includes internal pressure

[b]Load critical location

[c]Toughness critical location

TABLE 3-2

NORMAL CONDITION (DEAD WEIGHT + PRESSURE + THERMAL) LOADS FOR INDIAN POINT UNIT 2

Weld Location	Axial Load F_{xi} (Kips)[a]	Bending Moment M_b (in-Kips)
1[b]	1392	32588
2	1392	9090
3[c]	1456	16632
4[c]	1546	5671
5	1542	4230
6	1539	4582
7	1682	3654
8	1682	12125
9[c]	1878	22369
10	1375	6065
11	1375	4988
12[c]	1381	5483

[a] Includes internal pressure
[b] Load critical location
[c] Toughness critical locations

3-4
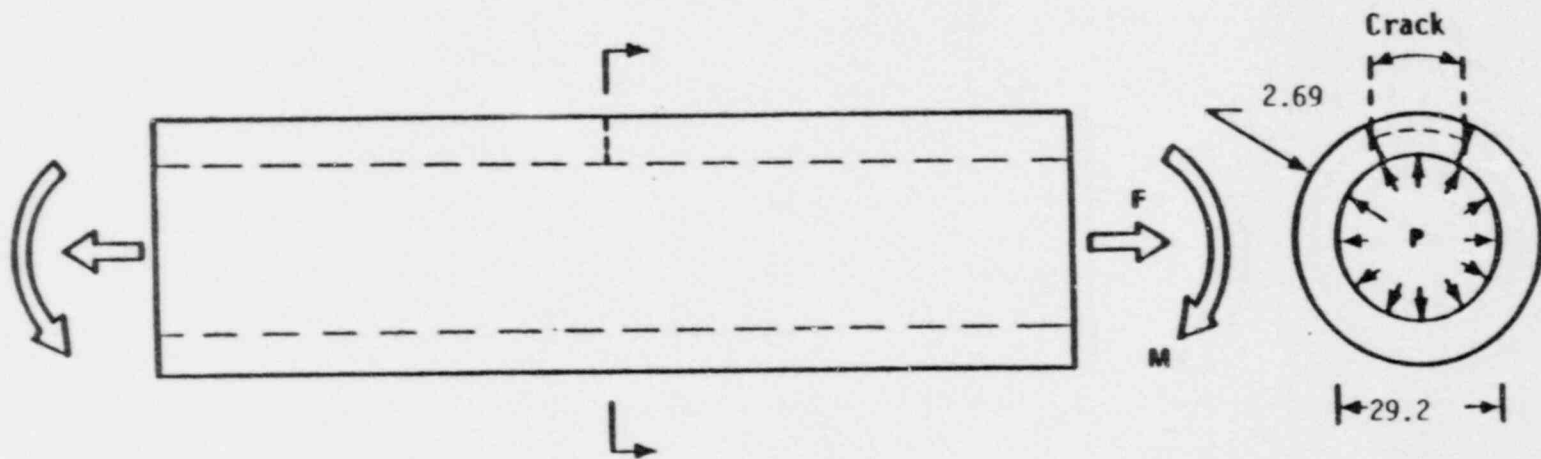
P = 2,235 psi
F = 1,768 kips
M = 38,913 in-kips

FIGURE 3-1 Reactor Coolant Pipe
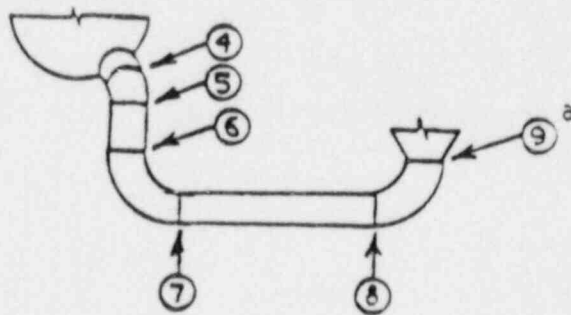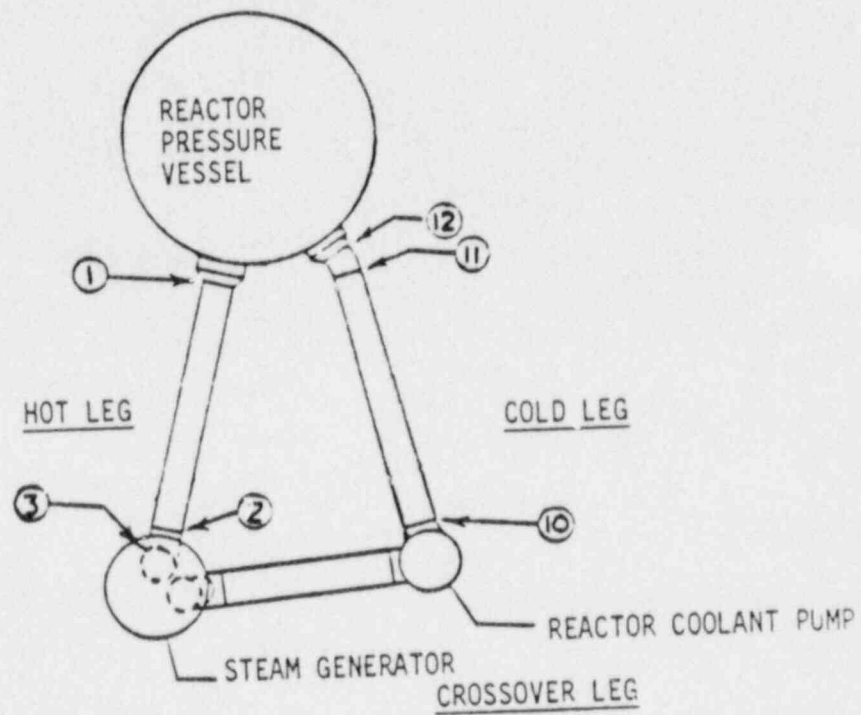
HOT LEG

    Temperature: 613°F; Pressure: 2235 psig

CROSSOVER LEG

    Temperature: 555°F; Pressure: 2200 psig

COLD LEG

    Temperature: 555°F; Pressure: 2290 psig

―――――――――――――――――――――

[a]For Loop 3, this location is designated 9A.

Figure 3-2 Schematic Diagram of Primary Loop Showing Weld Locations -
Indian Point Unit 2

4.0 FRACTURE MECHANICS EVALUATION

4.1 Global Failure Mechanism

Determination of the conditions which lead to failure in stainless steel
should be done with plastic fracture methodology because of the large amount
of deformation accompanying fracture. One method for predicting the failure
of ductile material is the plastic instability method, based on traditional
plastic limit load concepts, but accounting for strain hardening and taking
into account the presence of a flaw. The flawed pipe is predicted to fail
when the remaining net section reaches a stress level at which a plastic hinge
is formed. The stress level at which this occurs is termed as the flow
stress. The flow stress is generally taken as the average of the yield and
ultimate tensile strength of the material at the temperature of interest.
This methodology has been shown to be applicable to ductile piping through a
large number of experiments and will be used here to predict the critical flaw
size in the primary coolant piping. The failure criterion has been obtained
by requiring equilibrium of the section containing the flaw (Figure 4-1) when
loads are applied. The detailed development is provided in Appendix A for a
through-wall circumferential flaw in a pipe with internal pressure, axial
force, and imposed bending moments. The limit moment for such a pipe is given
by:

$$[\qquad\qquad\qquad\qquad\qquad] \quad a,c,e$$

where:

$$[$$

$$]^{a,c,e}$$

[

$$]^{a,c,e}$$

The analytical model described above accurately accounts for the piping internal pressure as well as imposed axial force as they affect the limit moment. Good agreement was found between the analytical predictions and the experimental results (Reference 8).

4.2 Local Failure Mechanism

The local mechanism of failure is primarily dominated by the crack tip behavior in terms of crack-tip blunting, initiation, extension and finally crack instability. Depending on the material properties and geometry of the pipe, flaw size, shape and loading, the local failure mechanisms may or may not govern the ultimate failure.

The stability will be assumed if the crack does not initiate at all. It has been accepted that the initiation toughness measured in terms of J_{Ic} from a J-integral resistance curve is a material parameter defining the crack initiation. If, for a given load, the calculated J-integral value is shown to be less than the J_{Ic} of the material, then the crack will not initiate. If the initiation criterion is not met, one can calculate the tearing modulus as defined by the following relation:

$$T_{app} = \frac{dJ}{da} \frac{E}{\sigma_f^2}$$

where:

T_{app} = applied tearing modulus

E = modulus of elasticity

σ_f = [   ]^{a,c,e} (flow stress)

a = crack length

[   ]^{a,c,e}

In summary, the local crack stability will be established by the two-step criteria:

$$J < J_{Ic}$$

or

$$T_{app} < T_{mat} \quad \text{if } J \geq J_{Ic}$$

4.3 Material Properties

The primary loop piping material for Indian Point Unit 2 is SA376-TP316, a wrought product form. The material for the primary loop fittings is SA351-CF8M, a cast product form. Welds exist as indicated in Figure 3-2. The minimum yield stress for these materials given in the ASME Code Section III, Division 1 are the same. The ultimate stress for the cast product form is somewhat less and is used in the analyses discussed in this report.

The tensile and flow properties of the load critical location and the toughness critical locations are given in Table 3-1.

The pre-service fracture toughness of cast materials in terms of J have been found to be very high at 600°F. Typical results are given in Figures 4-2 and 4-3 taken from References 9 and 10. J_{Ic} is observed to be over 2000 in-lbs/in^2. However, cast stainless steels are subject to thermal aging during service. This thermal aging causes an elevation in the yield strength of the material and a degradation of the fracture toughness, the degree of degradation being proportional to the level of ferrite in the material.

4-3

To determine the effects of thermal aging on piping integrity, a detailed study was carried out in Reference 10. In that report, fracture toughness results were presented for a material representative of [

]^{a,c,e} Toughness

results were provided for the material in the full service life condition and these properties are also presented in Figure 4-4 of this report for information. The J_{Ic} value for this material at operating temperature was approximately [   ]^{a,c,e} and the maximum value[a] of J obtained in the tests was in excess of [   ]^{a,c,e} The tests of this material were conducted on small specimens and therefore rather short crack extensions occurred, (maximum extension 4.3 mm) so it is expected that higher J values would be sustained for larger specimens. T_{mat} was [

]^{a,c,e} at operating temperature. The effects of the aging process on the end-of-service life fracture toughness is discussed in Appendix B.

End-of-service life toughnesses for the heats are established using the alternate toughness criteria methodology. By that methodology a heat of material is said to be as good as [   ]^{a,c,e} if it can be demonstrated that its end-of-service fracture toughnesses equal or exceed those of [

]^{a,c,e}. Of the twenty-eight heats examined in Appendix B, seventeen are below the initial governing criterion. Three of these are in the cold leg fitting to the pressure vessel (locations 11 and 12, location 12 having the highest loads). All four heats of the 40 degree crossover leg elbow are in this category (locations 4 and 5, having higher loads). Three of the eight heats for each half at the 90 degree crossover leg elbow without a flow splitter are also included (locations 6 and 7). The crossover leg elbow with a flow splitter into the pump has five heats with low toughness. These occur at locations 8 and 9 with location 9 having the highest loads. The lowest toughness occurs in one half of the elbow in loop 3 only (location 9A). Finally, there are two heats in the hot leg elbow

_____

(a) An additional supplementary criterion applied here is that $J \leq J_{max}$ where J_{max} is the maximum value of J obtained from J tests for the material in question.

(locations 2 and 3 with 3 having the highest loads). Location 6 and 7 were not specifically analyzed since the toughness is higher and the loads lower than either of the other crossover leg critical locations (4 and 9). The fracture toughness criteria to be used in the fracture mechanics evaluation, based on the alternate toughness methodology of Appendix B, are given in Table 4-1. These toughness values are the lowest of all heats occurring at that location.

Available data on aged stainless steel welds (References 10 and 11) indicate the J_{Ic} values for the worst case welds are of the same order as the aged material. However, the slope of the J-R curve is steeper, and higher J-values have been obtained from fracture tests (in excess of 3000 in-lb/in^2). The applied value of the J-integral for a flaw in the weld regions will be lower than that in the base metal because the yield stress for the weld materials is much higher at temperature[a]. Therefore, weld regions are less limiting than the cast material.

It is thus conservative to choose the end-of-service life toughness properties of [   ]^{a,c,e} as representative of those of the welds and the forged pipes. Also, such fittings having an end-of-service life KCU greater than that of [   ]^{a,c,e} are also conservatively assumed to have the properties of [   ]^{a,c,e}.

In the fracture mechanics analyses that follow, the fracture toughness properties given in Table 4-1 will be used as the criteria against which the applied fracture toughness values will be compared.

4.4 Results of Crack Stability Evaluation

Figure 4-5 shows a plot of the plastic limit moment as a function of through-wall circumferential flaw length in the hot leg of the main coolant piping (load critical location 1) . This limit moment was calculated for Indian

_____

(a) In this report all applied J values were conservatively determined by using base metal strength properties.

Point Unit 2 from data for a pressurized pipe at 2235 psi with an axial force of 1768 kips, operating at 613°F with ASME Code minimum tensile properties. The maximum applied bending moment of 38913 in-kips can be plotted on this figure and used to determine a critical flaw length, which is shown to be [   ]^{a,c,e} inches.

In Figures 4-6 through 4-9 plots of the plastic limit moment as a function of through-wall circumferential flaw length at the toughness critical locations of the main coolant pipe are given. These limit moments were calculated as above using the appropriate pressure, forces, and dimensions as given either in Table 3-1 or Figure 3-2 with bending moment as a parameter. The ASME Code minimum properties at 555°F were used. Critical flaw lengths were determined as in Figure 4-5 by use of the maximum applied bending moment. The critical flaw length in Figures 4-6 through 4-9 are all seen to exceed the [   ]^{a,c,e} inches established for load critical location 1.

At the load critical location a series of through-wall circumferential cracks were assumed to exist. Finite element elastic plastic fracture mechanics analyses were used applying faulted conditions loads to determine J_{app} for each flaw size. For a 7.5-inch through-wall circumferential flaw, J_{app} was found to be [   ]^{a,c,e} in-lb/in^2 which exceeds J_{Ic} but is less than J_{max}. Thence, the applied tearing modulus, T_{app}, was calculated and found to be [   ]^{a,c,e} which is a factor of over 6 below T_{mat} defined for this location in Section 4.3. Thus the flaw under consideration will remain stable and the critical flaw size exceeds 7.5 inches. Smaller flaw sizes were also examined. Significantly, a [   ]^{a,c,e} inch through-wall flaw yielded a J_{app} of [   ]^{a,c,e} in-lb/in^2 which is less than J_{Ic}.

The toughness critical locations were evaluated as follows. In Table 3-1, the outer surface axial stress (σ_a) at toughness critical location 9 (highest loads) is seen to be 18.4 ksi. Stresses due to the internal pressure of 2235 psi are as follows (see Reference 12):

σ_c (circumferential stress): 11.1 ksi

σ_r radial stress: 0

The von Mises effective stress, σ_{eff}, (see Reference 13) is given by

$$\sigma_{eff} = \frac{1}{\sqrt{2}} \sqrt{(\sigma_a - \sigma_r^2) + (\sigma_c - \sigma_r^2) + (\sigma_a - \sigma_c^2)}$$

and is 16.0 ksi.

Thus the effective stress is less than the yield stress and by the Von Mises plasticity theory yielding does not occur. Also, similar consideration at the other toughness critical locations confirms that yielding does not occur there. Hence, linear elastic fracture mechanics is applicable for analyzing the pipes with hypothesized flaws at the other toughness critical locations[a]. The analytical method used for the local stability evaluation at these locations is summarized below.

The stress intensity factors corresponding to tension and bending are expressed, respectively, by (see Reference 14)

$$K_t = \sigma_t \sqrt{\pi a} \; F_t(\alpha)$$
$$K_b = \sigma_b \sqrt{\pi a} \; F_b(\alpha)$$

where $F_t(\alpha)$ and $F_b(\alpha)$ are stress intensity calibration factors corresponding to tension and bending, respectively, a is the half-crack length, α is the half-crack angle, σ_t is the remote uniform tensile stress, and σ_b is the remote fiber stress due to pure bending. Data for $F_t(\alpha)$ and $F_b(\alpha)$

---

[a] At load critical location 1, discussed above, the effective stress is 22.6 ksi which exceeds the yield stress; thus the linear elastic method was not applied.

are given in Reference 14. The effect of the yielding near the crack tip can
be incorporated by Irwin's plastic zone correction method (see Reference 15)
in which the half-crack length, a, in these formulas is replaced by the
effective crack length, a_{eff}, defined by

$$a_{eff} = a + \frac{1}{2\pi} \frac{K^2}{\sigma_y^2}$$

for plane stress plastic corrections, where σ_y is the yield strength of
the material and K is the total stress intensity factor due to combined
tensile and bending loads (i.e., $K = K_t + K_b$). Finally, the J_{app}-value
is determined by the relation $J_{app} = K^2/E$, where E is Young's Modulus.

J_{app} was calculated for the five toughness critical locations using crack
length as a parameter. The results are presented in Table 7-1 of Chapter 7
wherein J_{app} values and leak rates are examined in assessing margin.

For J_{app} less than the local crack stability criterion given in Section 4.2,
the critical circumferential flaw lengths are at least 7.5 inches, [

]b,c,e at load critical

location 1 and toughness critical locations 3, 4, 9, and 12, respectively. At
toughness critical location 9A (one-half 90-degree pump inlet elbow on loop
3), the critical flaw length is [   ]a,c,e.

In summary, the critical flaw size has been shown to be [   ]a,c,e inches at
toughness critical location 9A while for all other locations the critical flaw
size exceeds 7.5 inches.

TABLE 4-1

FRACTURE TOUGHNESS CRITERIA USED IN THE
LEAK-BEFORE-BREAK EVALUATION

Location or Description	J_{Ic} (in-lb/in^2)	T_{mat}	J_{max} (in-lb/in^2)

a,c,e

---

[a] Included in this grouping are the heats at load critical location 1.
[b] The lowest of the values for all heats are given here.
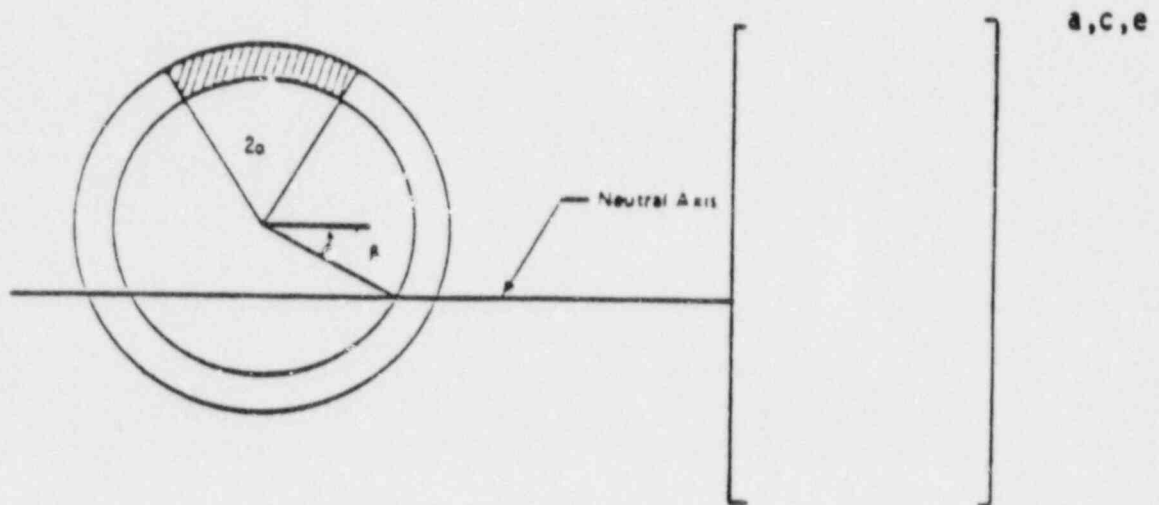[c] Properties for the worst of the two halves of the fitting.

a,c,e

2α

α

— Neutral Axis

FIGURE 4-1 [   ] a,c,e
STRESS DISTRIBUTION

a,c,e
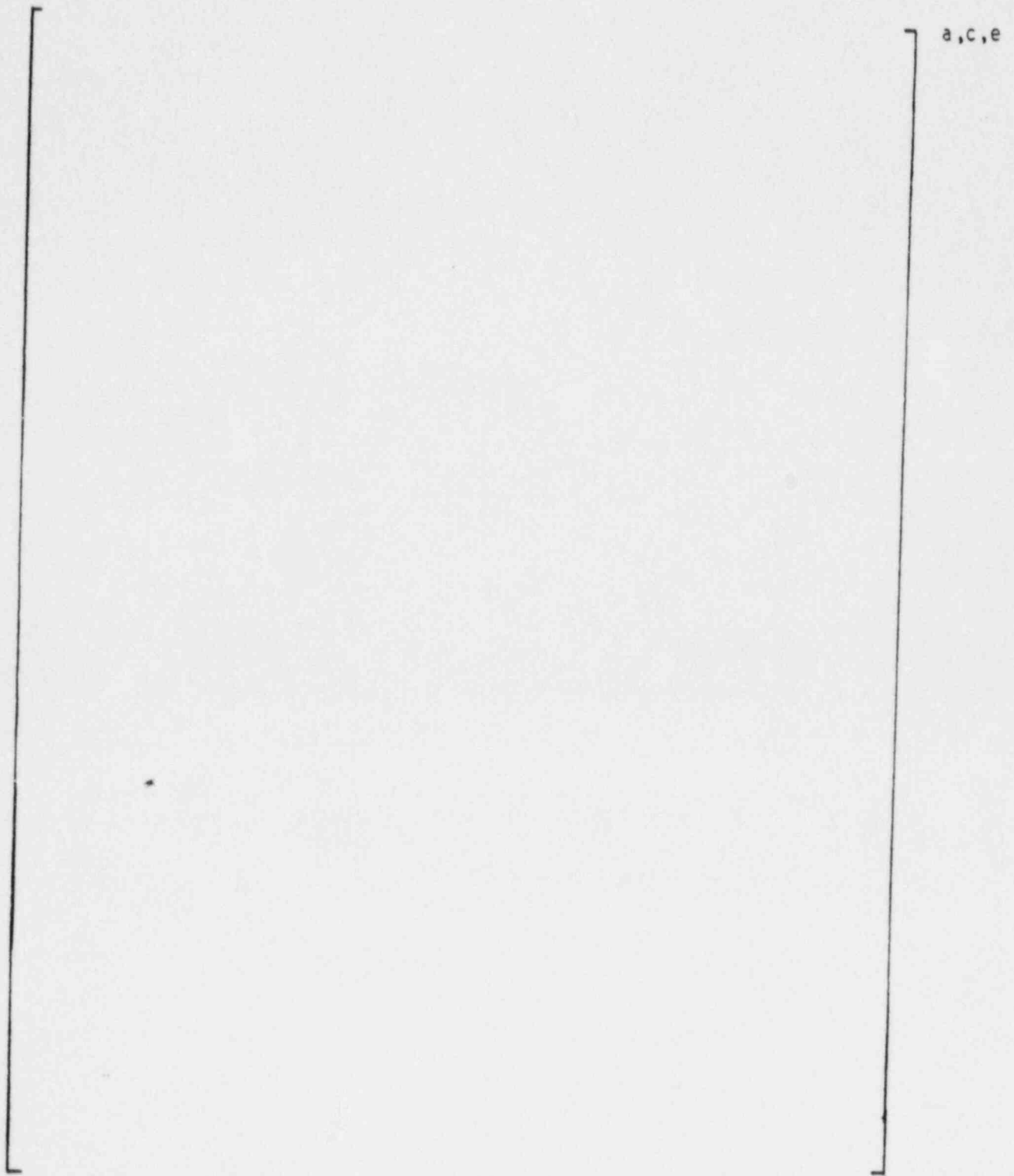
Figure 4-2   J vs Δa for SA376 TP316 Wrought Stainless Steel at 600°F

a,c,e

Figure 4-3 J vs Δa for SA351-CF8M Cast Stainless Steel at 600°F

]a,c, e

FIGURE 4-4   J-△a Curves at Different Temperatures for Aged Material [   ]a,c,e
             (7500 Hours at 400°C)

4-13

a,c,e

FLAW GEOMETRY

OD = 34.58 in
t = 2.69 in
p = 2235 psi
F = 1768 kips
σ_y = 18.7 ksi
σ_u = 67.0 ksi
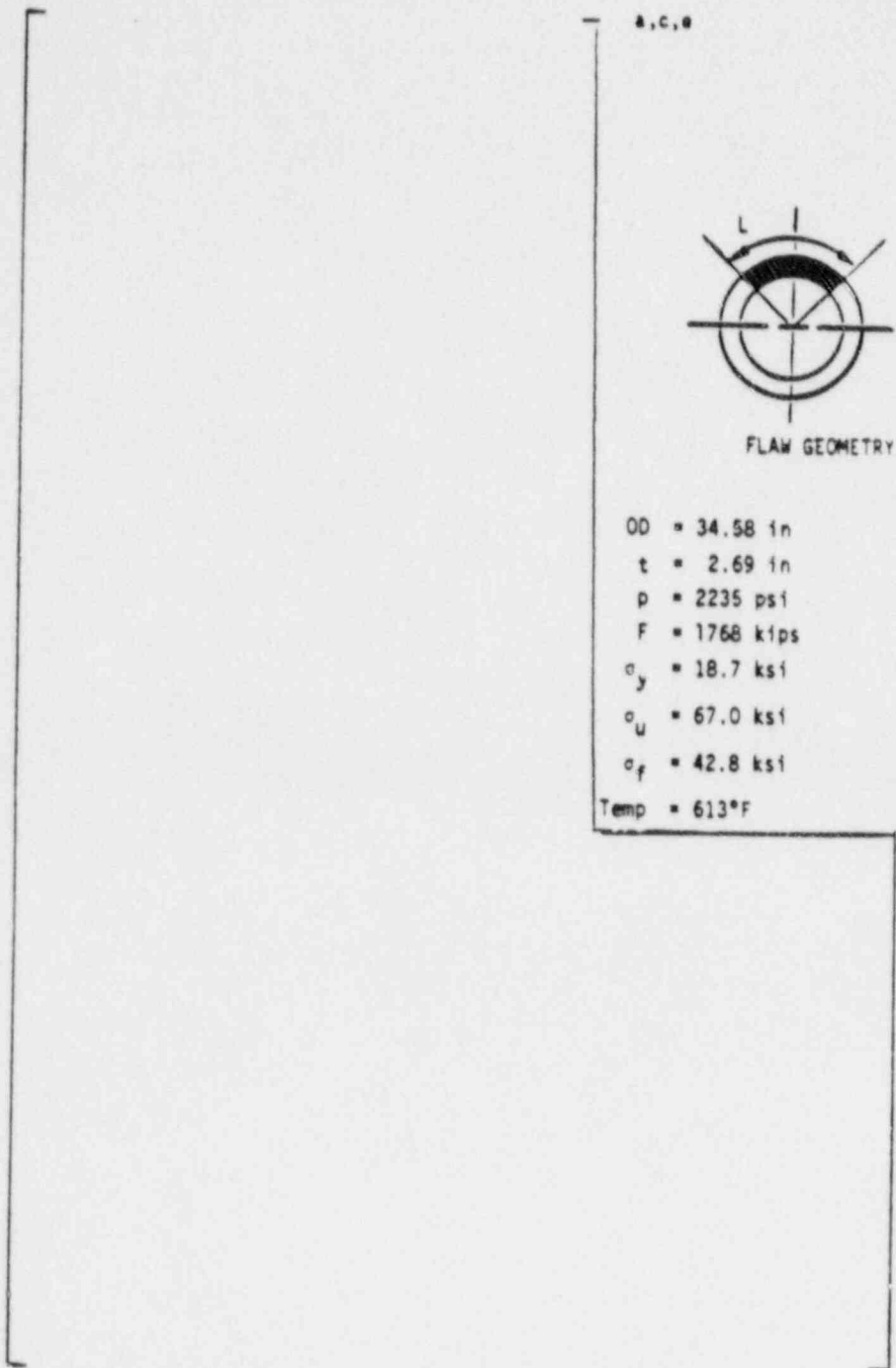σ_f = 42.8 ksi
Temp = 613°F

Figure 4-5 "Critical" Flaw Size Prediction - Hot Leg at Load Critical
         Location 1

4-14

FLAW GEOMETRY

OD – 36.96 in.
t = 2.88 in.
P = 2235 psi
F = 1724 kips
σ_y = 18.7 ksi
σ_u = 67.0 ski
σ_f = 42.8
Temp = 613°
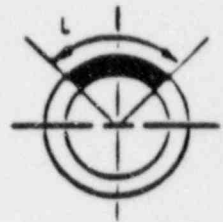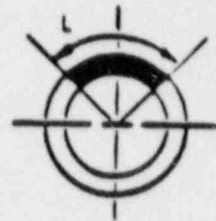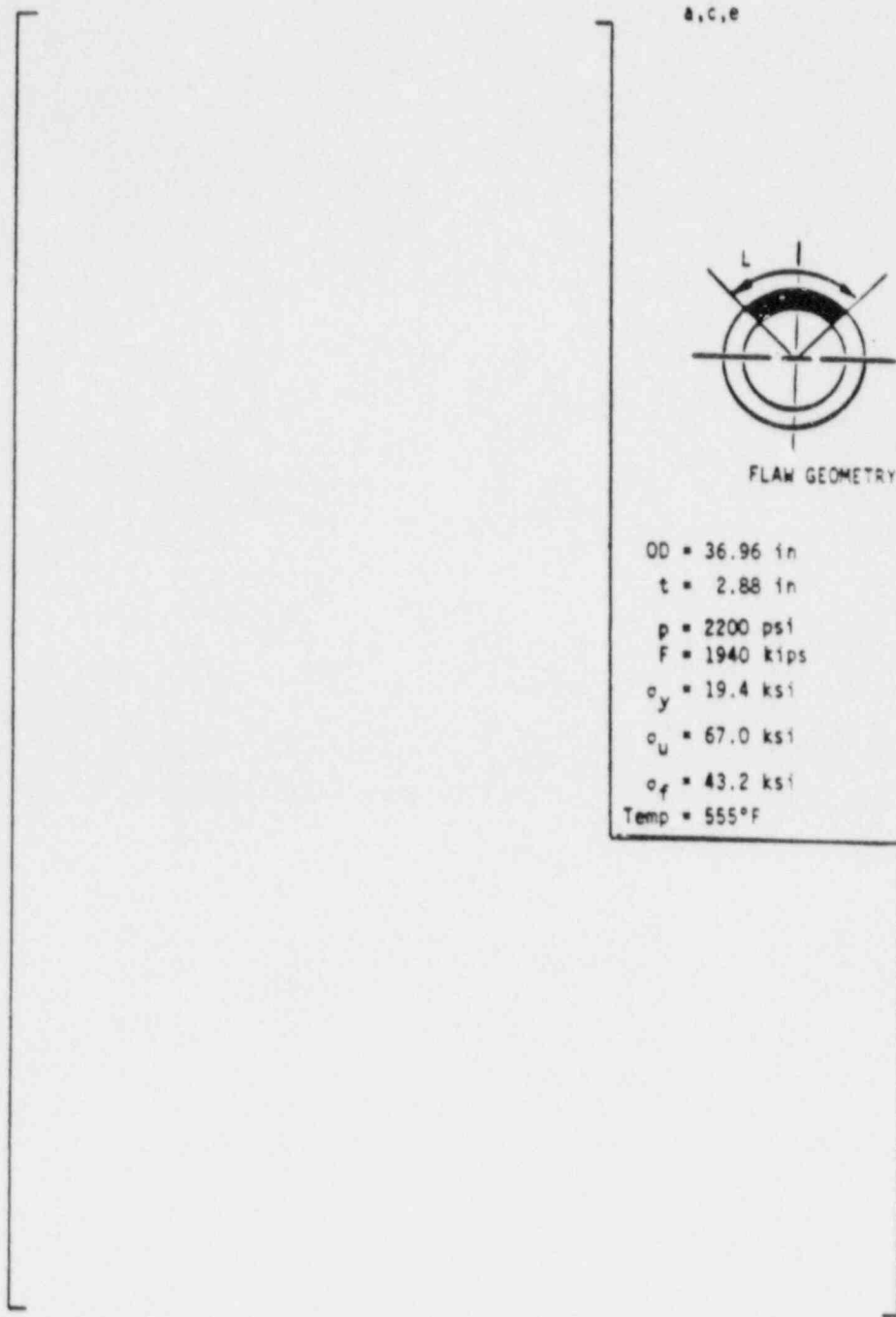
Figure 4-6   "Critical" Flaw Size Prediction – Hot Leg at Load Critical
            Location 3

FLAW GEOMETRY

OD = 36.96 in.
t = 2.88 in.
P = 2200 psi
F = 1715 kip
σ_y = 19.4 ksi
σ_u = 67.0 ksi
σ_f = 43.2 ksi
Temp = 555°F

Figure 4-7 "Critical" Flaw Size Prediction - Crossover Leg at Toughness
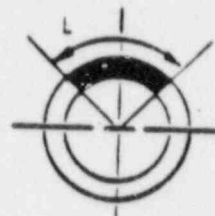Critical Location 4

a,c,e

FLAW GEOMETRY

OD = 36.96 in

t = 2.88 in

p = 2200 psi
F = 1940 kips

σ_y = 19.4 ksi

σ_u = 67.0 ksi

σ_f = 43.2 ksi

Temp = 555°F

Figure 4-8 "Critical" Flaw Size Prediction - Crossover Leg at Toughness
Critical Location 9

4-17

a,c,e

FLAW GEOMETRY

OD = 32.80 in
t = 2.55 in
p = 2290 psi
F = 1664 kips
σ_y = 19.4 ksi
σ_u = 67.0 ksi
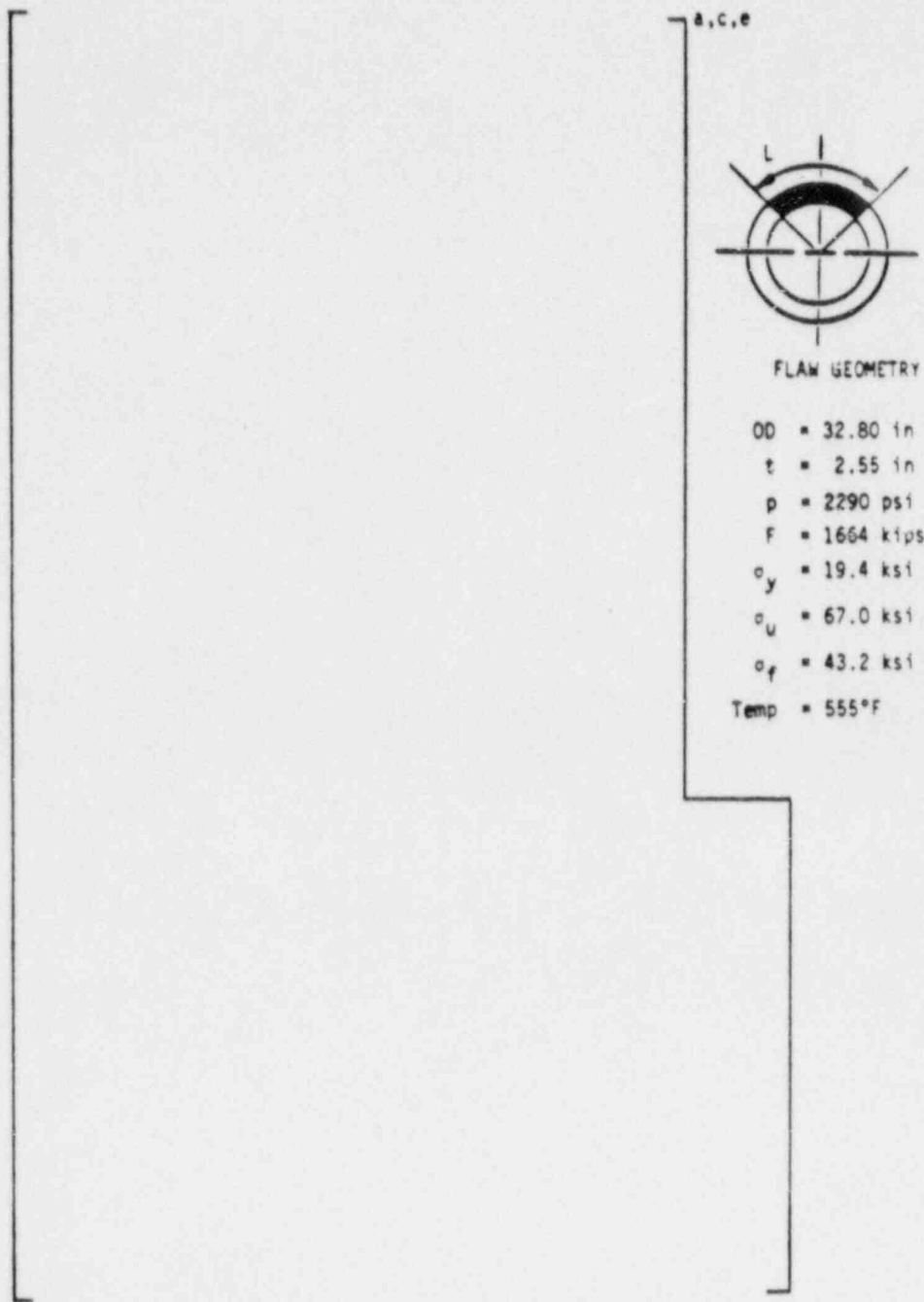σ_f = 43.2 ksi
Temp = 555°F

Figure 4-9   "Critical" Flaw Size Prediction - Cold Leg at Toughness
Critical Location 12

5.0 LEAK RATE PREDICTIONS

5.1 Introduction

Fracture mechanics analysis has shown that postulated through-wall cracks in
the primary loop would remain stable and not cause a gross failure of this
component. If such a through-wall crack did exist, it would be desirable to
detect the leakage such that the plant could be brought to a safe shutdown
condition. The purpose of this section is to discuss the method which will be
used to predict the flow through such a postulated crack and present the leak
rate calculation results for through-wall circumferential cracks.

5.2 General Considerations

The flow of hot pressurized water through an opening to a lower back pressure
causes flashing which can result in choking. For long channels where the
ratio of the channel length, L, to hydraulic diameter, D_H, (L/D_H) is
greater than [ ]^{a,c,e}, both [   ]^{a,c,e} must be
considered. In this situation the flow can be described as being single-phase
through the channel until the local pressure equals the saturation pressure of
the fluid. At this point, the flow begins to flash and choking occurs.
Pressure losses due to momentum changes will dominate for [   ]^{a,c,e}
However, for large L/D_H values, friction pressure drop will become important
and must be considered along with the momentum losses due to flashing.

5.3 Calculation Method

The basic method used in the leak rate calculations is the method developed by
[

]^{a,c,e}

The flow rate through a crack was calculated in the following manner. Figure
5-1 from Reference 16 was used to estimate the critical pressure, Pc, for the
primary loop enthalpy condition and an assumed flow. Once Pc was found for a
given mass flow, the [   ]^{a,c,e}

was found from Figure 5-2 taken from Reference 16. For all cases considered, since [   ]^{a,c,e} Therefore, this method will yield the two-phase pressure drop due to momentum effects as illustrated in Figure 5-3. Now using the assumed flow rate, G, the frictional pressure drop can be calculated using

$$\Delta P_f = [\qquad\qquad]^{a,c,e} \qquad\qquad\qquad (5-1)$$

where the friction factor f is determined using the [   ]^{a,c,e} The crack relative roughness, ε, was obtained from fatigue crack data on stainless steel samples. The relative roughness value used in these calculations was [   ]^{a,c,e} RMS.

The frictional pressure drop using Equation 5-1 is then calculated for the assumed flow and added to the [
            ]^{a,c,e} to obtain the total pressure drop from the primary system to the atmosphere. That is, for the primary loop

$$(5-2)$$

Absolute Pressure - 14.7 = [   ]^{a,c,e}

for a given assumed flow G. If the right-hand side of Equation 5-2 does not agree with the pressure difference between the primary loop and the atmosphere, then the procedure is repeated until Equation 5-2 is satisfied to within an acceptable tolerance and this results in the flow value through the crack. This calculational procedure has been recommended by [
            ]^{a,c,e} for this type of [
    ]^{a,c,e} calculation.

5.4 Leak Rate Calculations

Leak rate calculations were made as a function of crack length for all the critical locations previously identified. The normal operating loads of Table 3-2 were applied in these calculations. The crack opening area was estimated

using the method of Reference 14 and the leak rate was calculated using the two-phase flow formulation described above. The results are tabulated in Table 7-1 of Chapter 7 wherein J_{app} values and leak rates are examined in assessing margin.

The Indian Point Unit 2 plant has an RCS pressure boundary leak detection system which is consistent with the guidelines of Regulatory Guide 1.45 for detecting leakage of 1 gpm in one hour. For the critical flaw size at load critical location 1 in the hot-leg, a factor in excess of 120 exists between the calculated leak rate and the 1 gpm criteria of Regulatory Guide 1.45.

For the worst toughness critical location (9A), the largest stable flaw has a factor of over 20 above the 1 gpm criteria of Regulatory Guide 1.45. For the other toughness critical locations, the leak rate factors range from 43 to 195.
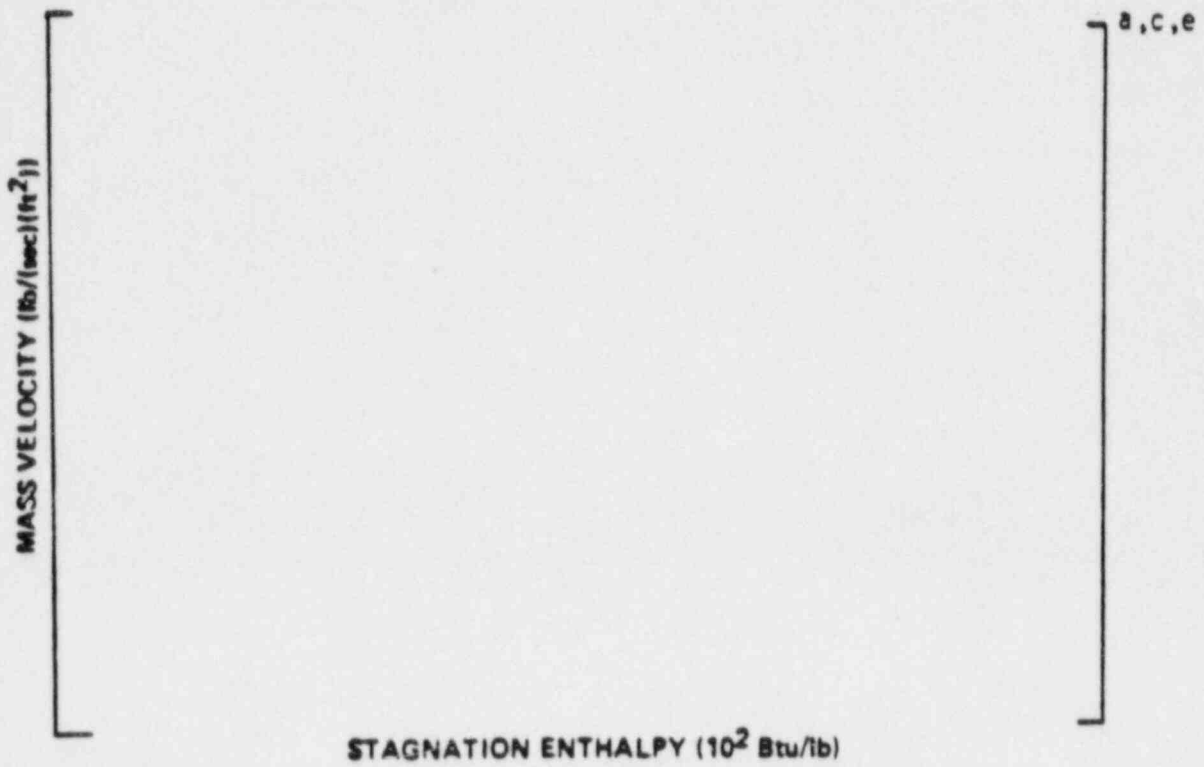
MASS VELOCITY (lb/(sec)(ft^2))

a,c,e

STAGNATION ENTHALPY (10^2 Btu/lb)

Figure 5-1   Analytical Predictions of Critical Flow Rates of Steam-
            Water Mixtures

CRITICAL PRESSURE RATIO (p_c/p_o)

a,c,e

LENGTH/DIAMETER RATIO (L/D)
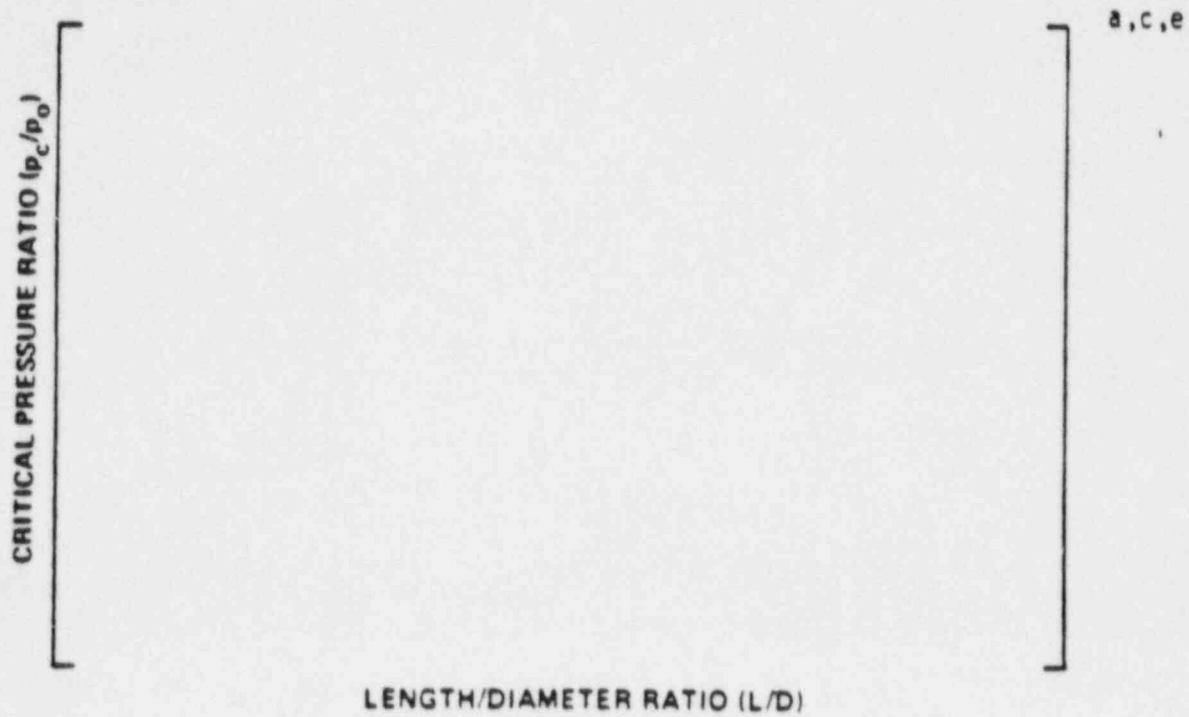
Figure 5-2 [   ]^{a,c,e} Pressure Ratio as a Function
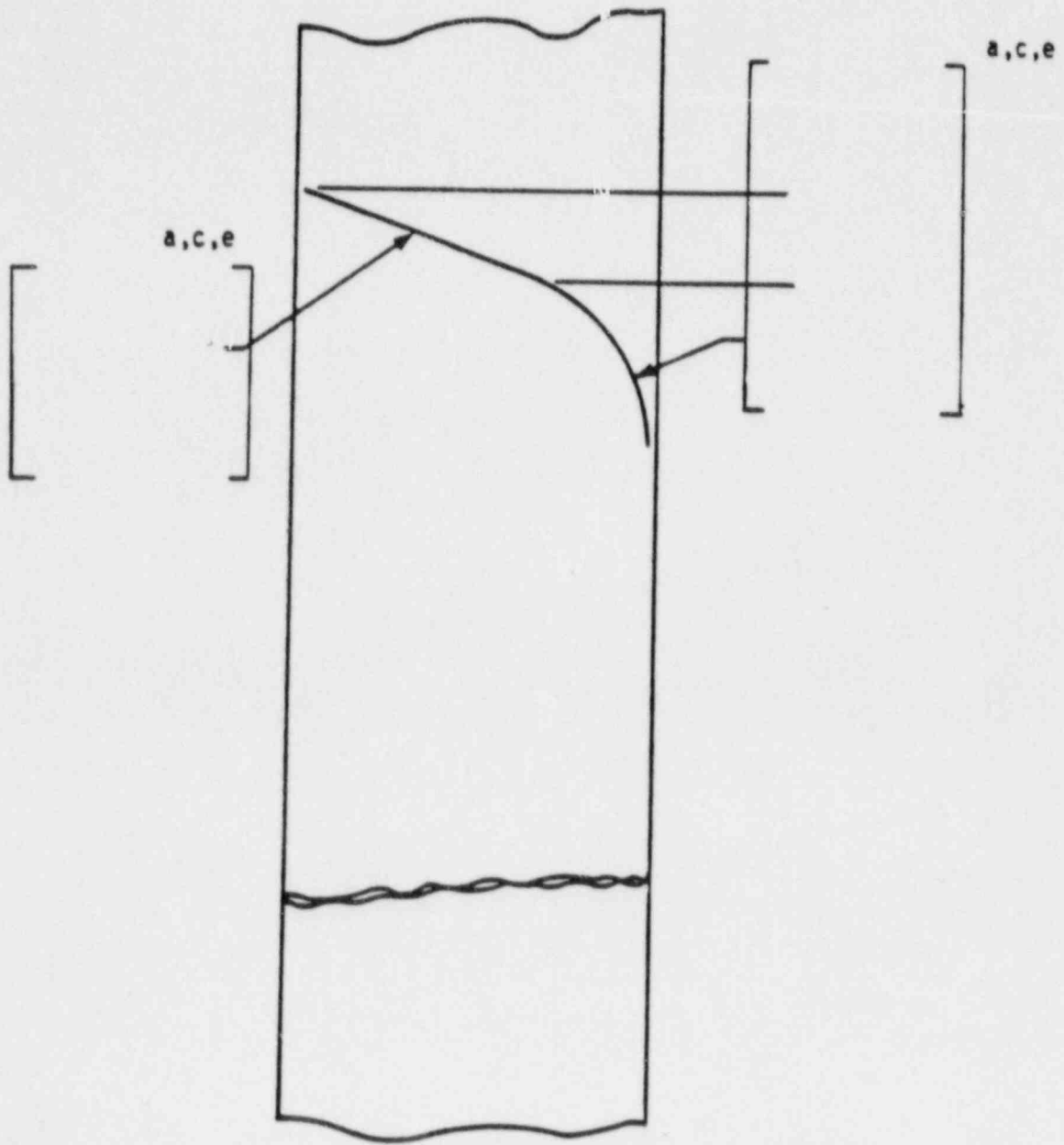   of L/D

a,c,e

a,c,e

Figure 5-3   Idealized Pressure Drop Profile Through a Postulated Crack

5-6

6.0 FATIGUE CRACK GROWTH ANALYSIS

To determine the sensitivity of the primary coolant system to the presence of small cracks, a fatigue crack growth analysis was carried out for the [

]^{a,c,e} region of a typical system (see Location
[   ]^{a,c,e} of Figure 3-2). This region was selected because crack growth calculated here will be typical of that in the entire primary loop. Crack growths calculated at other locations can be expected to show less than 10% variation. Thermal aging has been shown not to impact fatigue crack growth (References 10 and 11).

A [

]^{a,c,e} of a plant typical in geometry and operational characteristics to any Westinghouse PWR System. [

]^{a,c,e}

All normal, upset, and test conditions were considered and circumferentially oriented surface flaws were postulated in the region, assuming the flaw was located in three different locations, as shown in Figure 6-1. Specifically, these were:

    Cross Section A: [   ]^{a,c,e}
    Cross Section B: [   ]^{a,c,e}
    Cross Section C: [   ]^{a,c,e}

Fatigue crack growth rate laws were used [

]^{a,c,e} The law for stainless steel was derived from Reference 18, with a very conservative correction for the R ratio, which is the ratio of minimum to maximum stress during a transient. For stainless steel, the fatigue crack growth formula is:

$$\frac{da}{dn} = (5.4 \times 10^{-12})\ K_{eff}^{4.48}\ \text{inches/cycle}$$

where $K_{eff} = K_{max} (1-R)^{0.5}$

$R = K_{min}/K_{max}$

[

]a,c,e

[ ] a,c,e

where: [ ] a,c,e

The calculated fatigue crack growth for semi-elliptic surface flaws of circumferential orientation and various depths is summarized in Table 6-1, and shows that the crack growth is very small, regardless [
]a,c,e

TABLE 6-1

FATIGUE CRACK GROWTH AT [   ]a,c,e (40 YEARS)

INITIAL FLAW (IN)	FINAL FLAW (in)		
	[ ]a,c,e	[ ]a,c,e	[ ]a,c,e
0.292	0.31097	0.30107	0.30698
0.300	0.31949	0.30953	0.31626
0.375	0.39940	0.38948	0.40763
0.425	0.45271	0.4435	0.47421

$]^{a,c,e}$

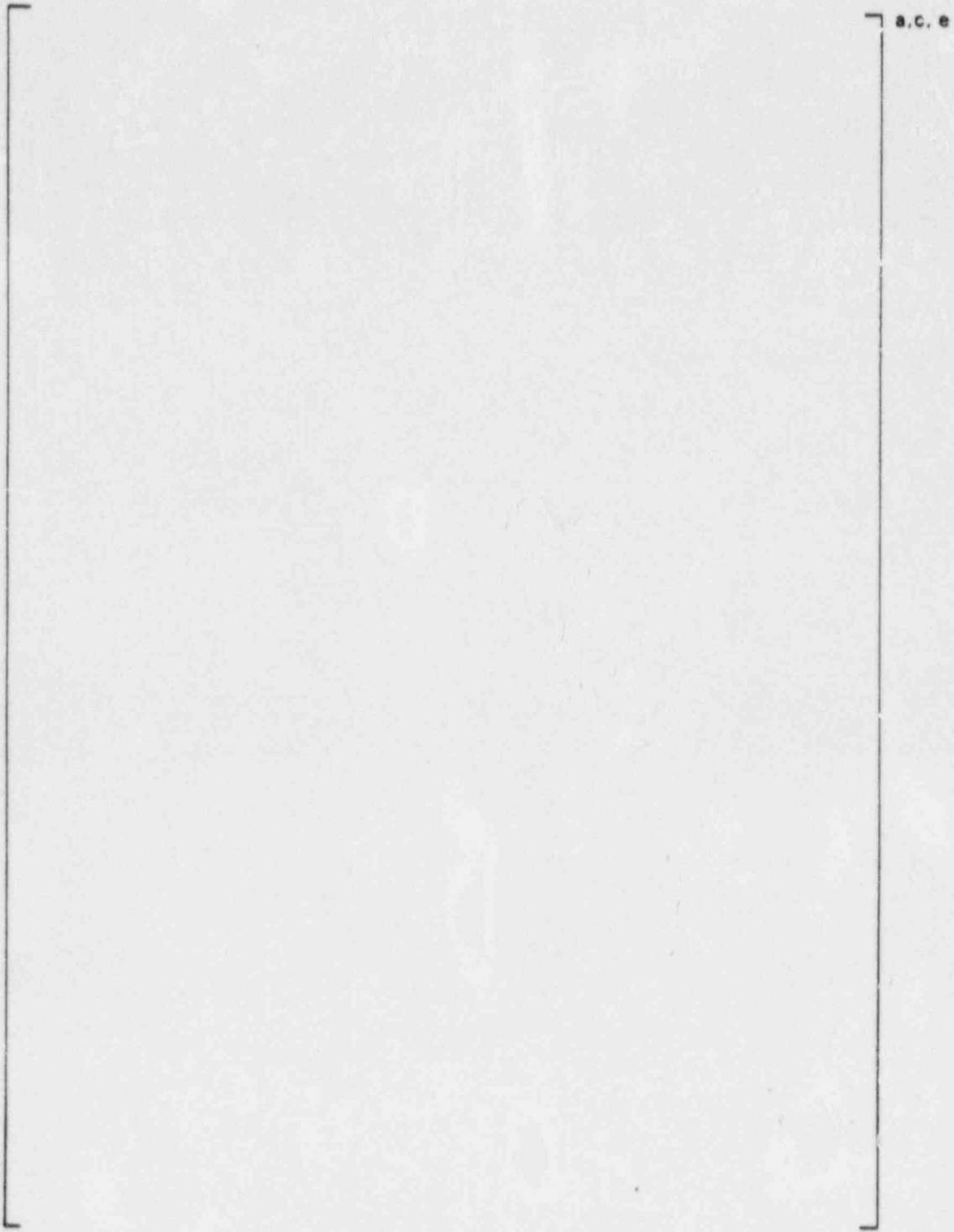Figure 6-1 Typical Cross-Section of [$]^{a,c,e}$

CRACK GROWTH RATE, da/dN (MICRO-INCHES/CYCLE)

a,c,e

Figure 6-2 Reference Fatigue Crack Growth Curves for [
]a,c,e

a,c, e

Figure 6-3 Reference Fatigue Crack Growth Law for [   ]a,c,e
in a Water Environment at 600°F

7.0 ASSESSMENT OF MARGINS

The results of the toughness and leak rate calculations for the five critical locations examined are summarized in Table 7-1. Margins for these critical locations are discussed below.

At load critical location 1 a 7.5 inch long through-wall circumferential flaw is seen to be stable exhibiting a $J_{app} < J_{max}$ and a T_{app} less than T_{mat} by over a factor of six. For a [ ]^{a,c,e} inch long flaw, J_{app} is less than J_{Ic}. For the toughness critical locations, the stable flaw sizes exceed the size at location 1 by a minimum of [ ]^{a,c,e} percent with one exception. For one-half of the crossover leg elbow at the pump in loop 3, toughness critical location 9A, the stable flaw size is [ ]^{a,c,e} inches. At all toughness critical locations, the stable flaw leak rates are well in excess of that required by Regulatory Guide 1.45.

As shown in Section 3.0, a margin of a factor of not less than 3 exists between calculated and ASME Code allowable faulted conditions and thermal stresses.

In Section 4.4, the "maximum" flaw sizes at load critical location 1 and the toughness critical locations are calculated using the limit load method and shown to be at least [ ]^{a,c,e} inches. Thus, based on the above, the "maximum" flaw sizes at these locations will, of course, exceed the stable crack lengths at their respective locations.

In Section 5, it is shown that at load critical location 1, a flaw of 7.5 inches would yield a leak rate in excess of 120 gpm. For a [ ]^{a,c,e} inch flaw, the leak rate is still adequate. Thus there is a margin of at least [ ]^{a,c,e} on flaw size.

At toughness critical locations 3, 4, 9, and 10, the corresponding margins on flaw size are at least [   ]^{a,c,e}, respectively. Even at the toughness critical location 9A, the margin on flaw size is near [   ]^{a,c,e} for a flaw leaking well in excess of that required by Regulatory Guide 1.45.

In summary, relative to:

1. Loads

   a. The J_{app} values for Indian Point Unit 2 are enveloped by the J values established from testing of highly aged material.

   b. Margins at the critical location of at least 3 on faulted conditions and thermal stresses exist relative to ASME Code allowable values.

2. Flaw Size

   a. Margins of near [   ]^{a,c,e} or greater on flaw size exist for stable flaw sizes with flow rates well in excess of a leak rate of 1 gal/min.

   b. If limit load is used as the basis for critical flaw size, the margin for global stability well exceeds that based upon fracture mechanics.

3. Leak Rate

   At load critical location 1, a margin in excess of 100 exists for the 7.5-inches long flaw between calculated leak rates and the 1 gpm criterion of Regulatory Guide 1.45. At the toughness critical locations, the margin on leak rate is at least 20 for flaws less than the unstable flaw size.

TABLE 7-1[a]

SUMMARY OF J_{app} AND LEAK RATE RESULTS
AS A FUNCTION OF CRACK LENGTH
AT THE SIX CRITICAL LOCATIONS

Location[b] (Loops)	Critical[c]			Crack Length (Inch)	J_{app}	T_{app}	Leak Rate (GPM)
	J_{Ic}	T_{mat}	J_{max}				
1 (1-4)				7.5		a,c,e	126 22 7.5
3 (1-4)							195[d] 10[d]
4 (1-4)							43 10
				7.5			
9 (1,2,4)							75[d] 10[d]
9A							21[d] 15[d] 5[d]
(3 only)							
12 (1-4)							50[d] 10[d]

a. J values have units of in-lb/in^2.

b. Location 1 is the load critical location, the remaining locations are toughness critical locations.

c. Values are lowest of all heats in indicated coolant loops.

d. For these locations, the flaw sizes for the leak rates are 7.5 inches or less.

8.0 CONCLUSIONS

This report justifies the elimination of RCS primary loop pipe breaks for the Indian Point Unit 2 plant as follows:

a. Stress corrosion cracking is precluded by use of fracture resistant materials in the piping system and controls on reactor coolant chemistry, temperature, pressure, and flow during normal operation.

b. Water hammer should not occur in the RCS piping because of system design, testing, and operational considerations.

c. The effects of low and high cycle fatigue on the integrity of the primary piping are negligible.

d. Adequate margins exist for ASME code allowable faulted and thermal loads.

e. Adequate margin exists between the leak rate of small stable flaws and the criterion of Reg. Guide 1.45.

f. Ample margin exists between the small stable flaw sizes of item e and larger stable flaws.

g. Ample margin exists in the material properties used to demonstrate end-of-service life (relative to aging) stability of the critical flaws.

For each critical location a flaw is identified (see Table 7-1) that will be stable throughout reactor life because of the ample margins in e, f, and g above and will leak at a detectable rate which will assure a safe plant shutdown.

Based on the above, it is concluded that RCS primary loop pipe breaks need not be considered in the structural design basis of the Indian Point Unit 2 plant.

9.0 REFERENCES

1. USNRC Generic letter 84-04, Subject: "Safety Evaluation of Westinghouse Topical Reports Dealing with Elimination of Postulated Pipe Breaks in PWR Primary Main Loops", February 1, 1984.

2. Letter from Westinghouse (E. P. Rahe) to NRC (R. H. Vollmer), NS-EPR-2768, dated May 11, 1983.

3. WCAP-9283, "The Integrity of Primary Piping Systems of Westinghouse Nuclear Power Plants During Postulated Seismic Events," March, 1978.

4. Letter Report NS-EPR-2519, Westinghouse (E. P. Rahe) to NRC (D. G. Eisenhut), Westinghouse Proprietary Class 2, November 10, 1981.

5. Letter from Westinghouse (E. P. Rahe) to NRC (W. V. Johnston) dated April 25, 1983.

6. Letter from Westinghouse (E. P. Rahe) to NRC (W. V. Johnston) dated July 25, 1983.

7. NUREG-0691, "Investigation and Evaluation of Cracking Incidents in Piping in Pressurized Water Reactors", USNRC, September 1980.

8. Kanninen, M. F., et. al., "Mechanical Fracture Predictions for Sensitized Stainless Steel Piping with Circumferential Cracks", EPRI NP-192, September 1976.

9. Landes, J. D., et. al., Fracture Toughness of 316 Stainless Steel Piping Material at 600°F, Westinghouse R&D Report 79-7D3-PIPRE-R1, May 17, 1979 (Westinghouse Proprietary Class 2).

10. WCAP-10456, "The Effects of Thermal Aging on the Structural Integrity of Cast Stainless Steel Piping For W NSSS," W Proprietary Class 2, November 1983.

11. Slama, G., Petrequin, P., Masson, S. H., and Mager, T. R.. "Effect of Aging on Mechanical Properties of Austenitic Stainless Steel Casting and Welds", presented at SMiRT 7 Post Conference Seminar 6 - Assuring Structural Integrity of Steel Reactor Pressure Boundary Components, August 29/30, 1983, Monterey, CA.

12. Durelli, A. J., et. al., Introduction to the Theoretical and Experimental Analysis of Stress and Strain, McGraw Hill Book Company, New York, (1958), pp 233-236.

13. Johnson, W. and Mellor, P. B., Engineering Plasticity, Van Nostrand Relmhold Company, New York, (1973), pp 83-86.

14. Tada, H., "The Effects of Shell Corrections on Stress Intensity Factors and the Crack Opening Area of Circumferential and a Longitudinal Through-Crack in a Pipe," Section II-1, NUREG/CR-3464, September 1983.

15. Irwin, G. R., "Plastic Zone Near a Crack and Fracture Toughness," Proc. 7th Sagamore Conference, P. IV-63 (1960).

16. [

                                    ]a,c,e

17. [
        ]a,c,e

18. Bamford, W. H., "Fatigue Crack Growth of Stainless Steel Piping in a Pressurized Water Reactor Environment," Trans. ASME Journal of Pressure Vessel Technology, Vol. 101, Feb. 1979.

19. [

    ]a,c,e

20. [

    ]a,c,e

21. Witt, F. J. and Kim, C. C., Toughness Criteria for Thermally Aged Cast Stainless Steel, Westinghouse Proprietary Class 2 Report WCAP 10931, Revision 1, July 1986.

APPENDIX A

LIMIT MOMENT

[

] a,c,e

a,c,e

FIGURE A-1 PIPE WITH A THROUGH-WALL CRACK IN BENDING

APPENDIX B

ALTERNATE TOUGHNESS CRITERIA FOR THE
INDIAN POINT UNIT 2 CAST PRIMARY LOOP COMPONENTS

B.1 INTRODUCTION

Not all of the individual cast piping components of the Indian Point Unit 2 primary loop piping satisfy the original [ ]^{a,c,e} criteria (Reference 10). In this appendix, the alternate toughness criteria for thermally aged cast stainless steel developed in Reference 21 will be used to categorize the various individual cast piping components thus establishing criteria based upon which the mechanistic pipe break evaluation may be performed. First the chemistry and calculated KCU values are given followed by an identification of each of the heats of material with a specific loop and location. The criteria for the various individual loop components are tabulated.

B.2 CHEMISTRY AND KCU TOUGHNESS

The correlation of Reference 11 which is based on the chemistry of the cast stainless steel piping was used to calculate the associated KCU value. The chemistry and end-of-service life KCU toughness values are given in Table B-1. Of the twenty-eight heats of cast stainless steel, seventeen fail to meet the current [ ]^{a,c,e} criteria. These heats occur in the fittings of the hot, cold and crossover legs in each of the four reactor loops.

B.3 THE AS-BUILT INDIAN POINT UNIT 2 LOOPS

Indian Point Unit 2 is a four-loop Westinghouse type pressurized water reactor plant. A typical four-loop primary system is sketched in Figure B-1. The four loops are identified as Loops 1, 2, 3 and 4 in Indian Point Unit 2. Sketches for associating piping component with specific locations and loop are given in Figures B-2 through B-4. The individual components are identified by heat numbers. The components which have toughnesses less than that of [ ]^{a,c,e} are identified (see Figures B-2 to B-4).

B.4 ALTERNATE TOUGHNESS CRITERIA FOR THE INDIAN POINT UNIT 2 CAST
PRIMARY LOOP MATERIAL ON A COMPONENT-BY-COMPONENT BASIS

The alternate toughness criteria for the Indian Point Unit 2 cast primary loop
material may be obtained by applying the methodology of Reference 21 to Table
B-1. First, it is observed that eleven of the 28 heats fall into [
]^{a,c,e}, i.e., they are as tough as [   ]^{a,c,e} The remaining heats fall
into [   ]^{a,c,e} with one in [   ]^{a,c,e}. The toughness
criteria for all 28 heats are given in Table B-2.

Loop 3 cold leg Heat No. [   ]^{a,c,e} has the lowest calculated
end-of-service life KCU at room temperature of [   ]^{a,c,e} daJ/cm^2 which
falls below that of [   ]^{a,c,e}. The δ-ferrite content is
[   ]^{a,c,e}. By Reference 21, the [

                                           ]^{a,c,e}.

Thus, for full-embrittlement

$J_{Ic} = [$ $]^{a,c,e}$

$T_{mat} = [ ]^{a,c,e}$

$J_{max} = [$ $]^{a,c,e}$

and

$KCU < [$ $]^{a,c,e}$

Since the end-of-service life KCU value is less than the full-embrittlement
KCU value, Heat No. [   ]^{a,c,e} is a [   ]^{a,c,e} as
defined in Reference 21 and the end-of-service life fracture toughness is [
                                           ]^{a,c,e}. These
results are given in Table B-2 for [   ]^{a,c,e}.

An example calculation for a [   ]a,c,e heat is given below. Similar
calculations for the remaining fifteen [   ]a,c,e heats were made.

The example calculation will be made for Heat [   ]a,c,e. The ferrite
content is [   ]a,c,e and the end-of-service life KCU is [   ]a,c,e
daJ/cm². The [

               ]a,c,e. Since the end-of-service life KCU exceeds the
fully aged KCU, the heat falls into [   ]a,c,e. Thus:

J_{Ic} = [

               ]a,c,e

T_{mat} = [

               ]a,c,e

and

J_{max} = [
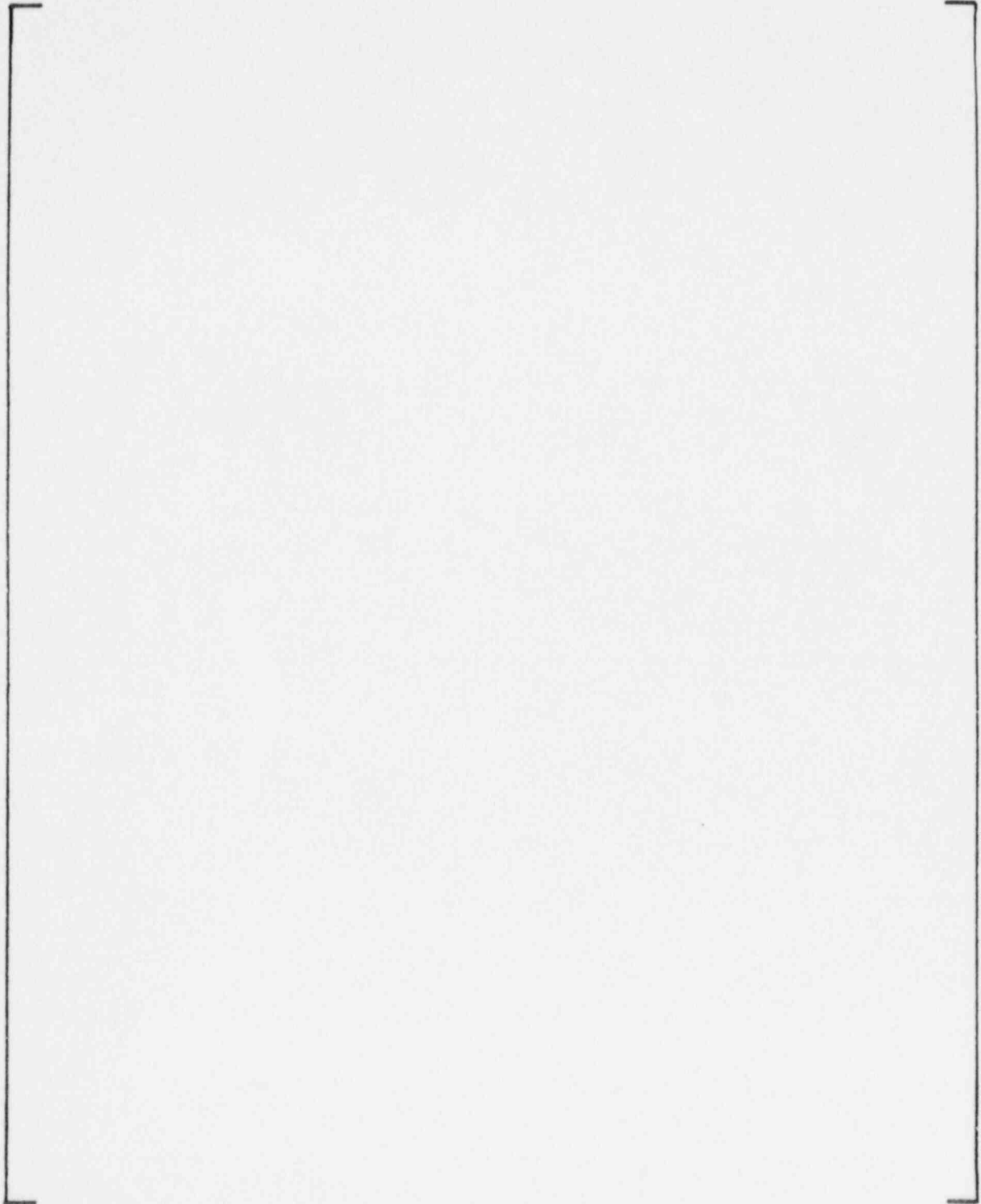
               ]a,c,e

TABLE B-1 Chemical and Physical Properties of Indian Point Unit 2 Cast Primary Loop Material - SA 351/CF8M

a,c,e

TABLE B-2

FRACTURE TOUGHNESS CRITERIA FOR THE CAST PRIMARY PIPING COMPONENTS OF THE INDIAN POINT UNIT 2 NUCLEAR PLANT
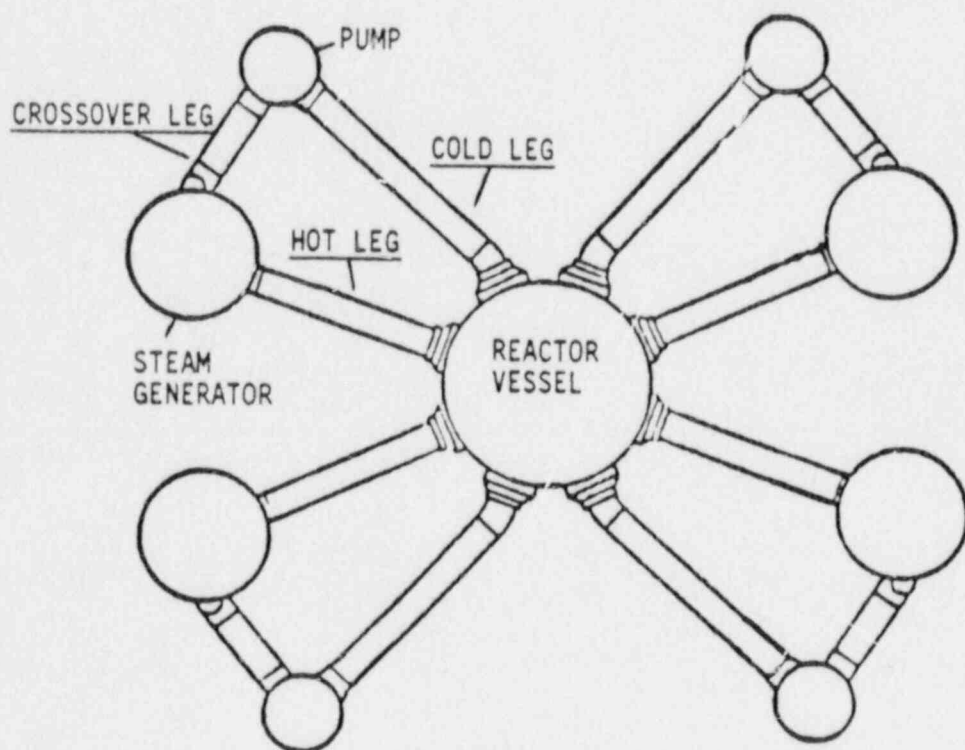
a,c,e

Figure B-1   Typical Layout of the Primary Loops for a Westinghouse
Four-Loop Plant Without Isolation Valves

a,c,e
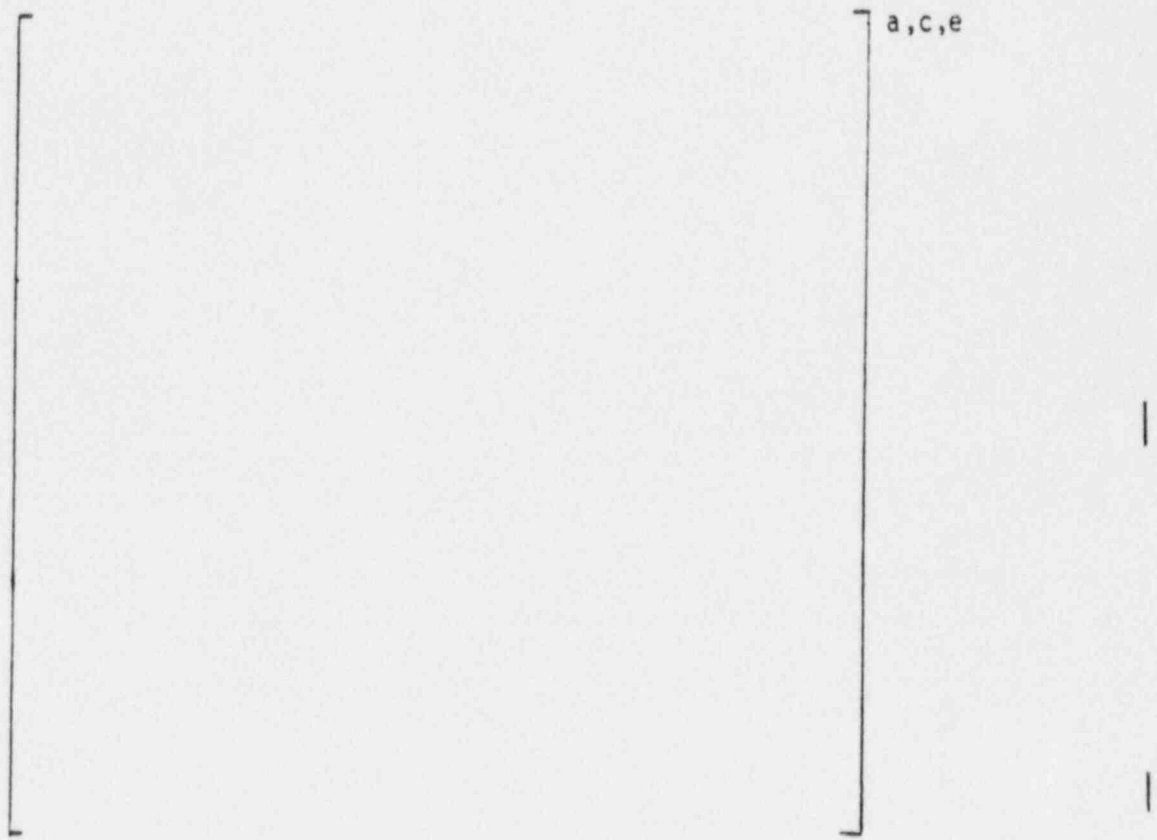
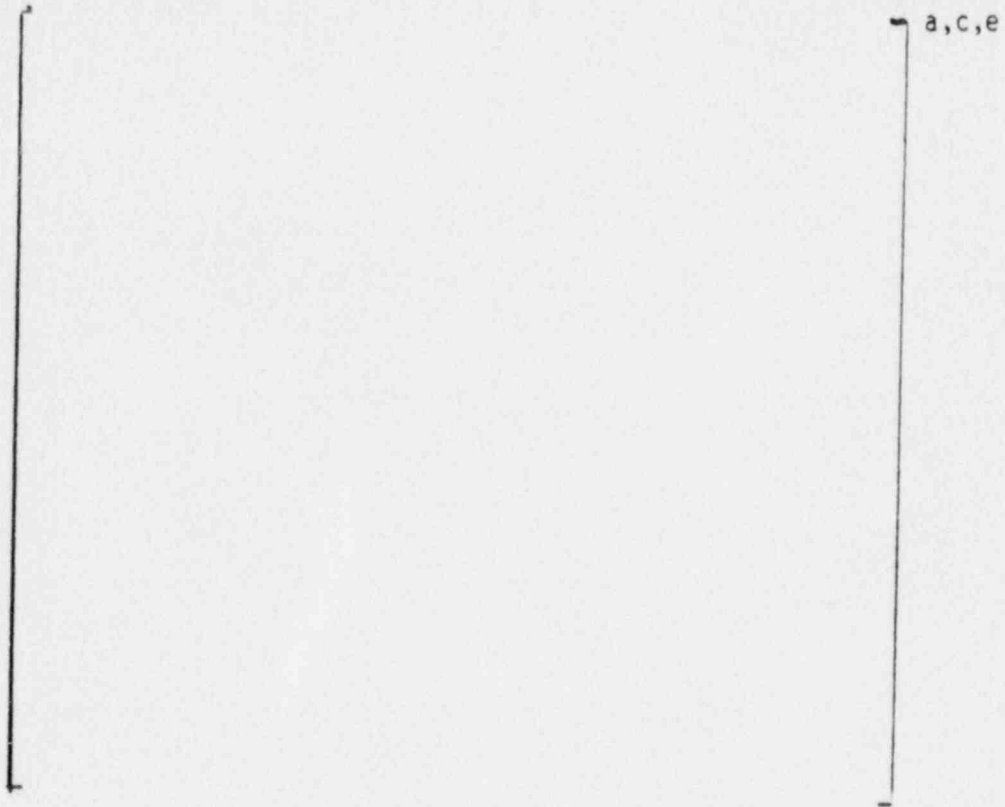Figure B-2   Identificati⹀ of Heats with Location for Cold Leg

a,c,e

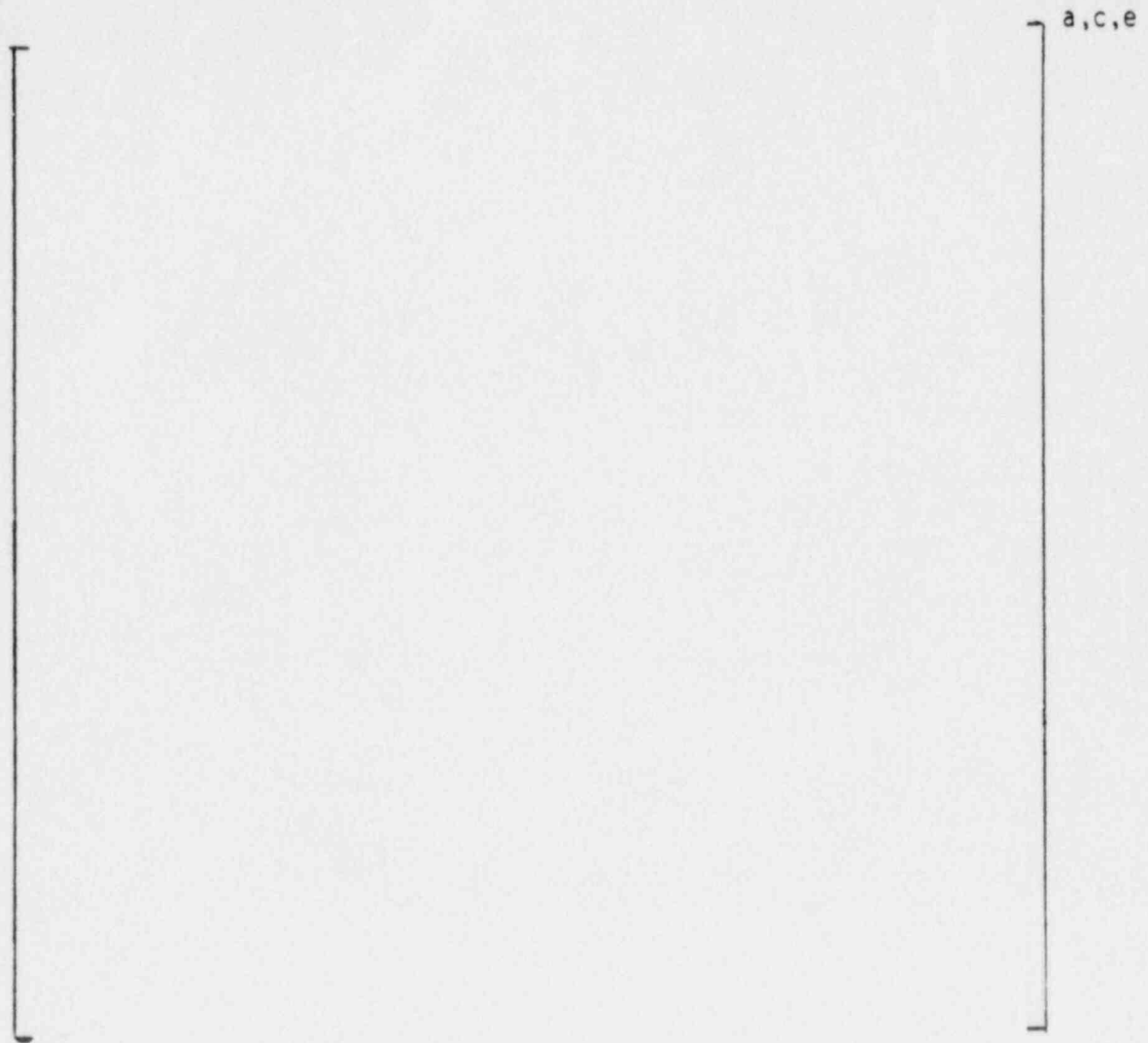Figure B-3   Identification of Heats with Location for Hot Leg

a,c,e

Figure B-4   Identification of Heats with Location for Crossover Leg

IPP-88-788

May 18, 1988

Mr. S. Sinha
Consolidated Edison Co. of New York, Inc.
4 Irving Place
New York, NY 10003

CONSOLIDATED EDISON COMPANY OF NEW YORK, INC.
INDIAN POINT 2
WCAP 10977 - Rev. 2
Editorial Corrections

Dear Mr. Sinha:

Two corrections to WCAP 10977-Rev. 2, "Technical Basis for Eliminating
Large Primary Loop Pipe Rupture as the Design Basis for Indian Point 2",
have been made. Both corrections are of an editorial nature and are as
follows:

1. Page 4-15, in the figure caption, Load should be replaced
    by Toughness.

2. Page 7-2, first line, replace 10 by 12.

Corrected versions of these pages are attached for both the Westinghouse
Proprietary Class 2 Report (WCAP-10977, Revision 2) and Westinghouse Class
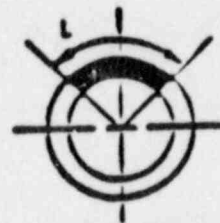3 Report (WCAP-10976, Revision 2).

Please incorporate them in your reports. Should you have any questions,
please call.

Very truly yours,

J. R. Gasperini, Project Engineer
New York Area
Operating Plant Projects

JRG/cda

cc: M. Marina
     G. Meyer
     M. Miele

FLAW GEOMETRY

OD = 36.96 in.
t = 2.88 in.
P = 2235 psi
F = 1724 kips
σ_y = 18.7 ksi
σ_u = 67.0 ski
σ_f = 42.8
Temp = 613°

Figure 4-6 "Critical" Flaw Size Prediction - Hot Leg at Toughness
Critical Location 3